Chaotic Spacetime: Fractal Sets in the Mixmaster Universe

Steve Flammia
(Dated: May 20, 2004)

I. INTRODUCTION

When a physical system is described by nonlinear equations of motion, the complex phenomenon known as *chaos* often results. By chaos it is meant that the systems dynamics are so complicated and so dependent on small uncertainties that any attempt at predicting the future behavior of the system is futile. Einstein's theory of General Relativity is governed by a set of equations that are nonlinear, especially when spacetime is highly curved. Thus, one might expect that near singularities the dynamics of spacetime is chaotic. In this paper, we focus on a specific model known as the mixmaster universe and study the behavior near the singularity at the big bang.

If one is to prove the existence of chaos in a General Relativistic setting, then one must deal with the additional constraint that the proof remain valid for all observers. Standard indicators of chaos such as the Lyapunov exponent or the metric entropy have been shown to be observer *dependent*, and are thus unsuitable for use in GR. Fractals, however, are fundamentally observer independent because they are self-affine (self-similar). The existence of fractal sets in the phase space of the mixmaster universe would then conclusively prove that the dynamics are chaotic.

The paper is organized as follows: in section II we describe the mixmaster universe and the discrete-time approximation of the dynamics; in section III A we prove that the set of fixed points for the discrete approximation is a repeller; in section IV we prove that the repeller is a fractal set, and thus the mixmaster universe is chaotic; in section V we discuss the emergence of a new fractal set in the discrete dynamics that (to the best of the author's knowledge) has not yet been discussed in the literature. We conclude in section VI. All though no formal citations are given during the course of the paper, a brief discussion of the literature that was consulted can be found in section VII. In Appendix A, the Mathematica code used to calculate all of the figures and quantities presented in this paper is listed. The figures are placed at the end of the paper.

II. THE MIXMASTER UNIVERSE

The metric for the mixmaster universe is

$$g = a^2 dx^2 + b^2 dy^2 + c^2 dz^2 - dt^2 \ , \tag{1}$$

where the factors a, b, c are scaling factors which depend only on time. Thus, the mixmaster universe is a homogeneous universe (a, b, c independent of x, y, z), but it is in general anisotropic. If we let $a = b = c$, we recover the Friedman-Robertson-Walker cosmology, which is of course isotropic.

The vacuum Einstein equations lead directly to the following equations for the scaling parameters:

$$2(\ln a)'' = (b^2 - c^2)^2 - a^4 \ , \ \text{cyclic}(a, b, c) \tag{2}$$

where the prime denotes differentiation with respect to a time τ which is related to the cosmic time by $dt = abc\, d\tau$.

Solving for the dynamics for the complete system (numerically, or course) shows that the volume of the universe expands from a big bang, reaches a maximum, and then contracts, ending in a big crunch. Near the singularities, the axes undergo "oscillations" and "bounces". The oscillations occur when one axis decreases monotonically while the others alternate between expanding and contracting. After some time in an oscillation epoch, the universe bounces, after which the axes permute roles and the oscillatory behave resumes. The cycles of bounces and oscillations occur an infinite number of times on the approach to the singularity.

If we consider the right hand side of equations (2) to be a potential, then the bounce phase can be considered as a scattering problem, with the universe scattering off the potential. When this potential is small, the Kasner metric

$$g = t^{2p_1}dx^2 + t^{2p_2}dy^2 + t^{2p_3}dz^2 - dt^2 \ , \tag{3}$$

gives a good description of the dynamics. Here the parameters p_i satisfy the constraints

$$\sum p_i = \sum p_i^2 = 1 \, . \tag{4}$$

By applying these constraints, we can reduce this to a one parameter problem:

$$\begin{aligned} p_1 &= \frac{-u}{1+u+u^2} \, , \\ p_2 &= \frac{1+u}{1+u+u^2} \, , \\ p_3 &= \frac{u+u^2}{1+u+u^2} \, , \end{aligned} \tag{5}$$

where the parameter u is constrained to lie in the interval $[1, \infty)$. As the reader may easily verify, equations (5) satisfy the constraints (4), as well as $p_1(u) = p_1(1/u)$, $p_2(u) = p_3(1/u)$, $p_3(u) = p_2(1/u)$, and $p_1 < p_2 < p_3$.

Since the Kasner metric is a good description when the potential is small, we can consider only the change in the parameter u after the universe has scattered off the potential, and in this way we can reduce the dynamics of equations (2) to a discrete map.

III. DISCRETE DYNAMICS: THE FAREY MAP

To obtain the discrete time evolution of the mixmaster universe, we use the evolution rules for the u parameter that were first characterized by Khalatnikov and Lifshitz:

$$f(u_n) = u_{n+1} = \begin{cases} u_n - 1 & , \, u \geq 2 \\ \dfrac{1}{u_n - 1} & , \, u < 2 \, . \end{cases} \tag{6}$$

To make this map time reversible, we allow the map to be two dimensional, and combine the map (7) with it's inverse map to construct the Farey map, defined as

$$F(u,v) = \begin{cases} (u-1, v+1) & , \, u \geq 2 \\ \left(\dfrac{1}{u-1}, \dfrac{1}{v} + 1\right) & , \, u < 2 \, . \end{cases} \tag{7}$$

This is the discrete version of the mixmaster universe which describes the dynamics except during the "bounce" phases. The map ignores the dynamics during the bounce, and instead calculates u immediately after the bounce, i.e. when the potential becomes negligible and the universe is again coasting in a Kasner phase of oscillations.

To show that this map is chaotic in a coordinate independent way, we find the strange repeller of this map, and show that it is a fractal set. A strange repeller is a set that is chaotic, nonattracting, and invariant (composed of fixed points).

A. Fixed Points of the Farey Map

To find the fixed points of the Farey map, we first note that since u and v are mapped inverse to one another, the set of fixed points is the same in both variables. Thus, if u_0 is a fixed point of the Farey map for arbitrary v, and v_0 is a fixed point for arbitrary u, then the pair (u_0, v_0) is a fixed point of the Farey map. We therefore find the fixed points of the reduced map f of equation (6), which we redefine in terms of two submaps so that

$$f(u) = \begin{cases} O(u) & , u \geq 2 \\ B(u) & , u < 2 \, , \end{cases} \tag{8}$$

where the maps O and B are defined as

$$O(u) = u - 1 \quad , \quad B(u) = \frac{1}{u-1} \, . \tag{9}$$

As one might guess from the names, the O map describes the evolution during an oscillation epoch, and the B map describes the shift in the u parameter immediately after the scattering (bounce) phase of the mixmaster evolution.

The set of fixed points of the map f are the set of points w satisfying the equation

$$f^k(w) = w \ , \quad k = 1, 2, \ldots \quad . \tag{10}$$

The set of fixed points of order k has an elegant solution in terms of something called the irrational Farey tree (hence the name "Farey map"), but unfortunaly a discussion of this lies beyond the scope of this paper. For now, it suffices to know that the set of fixed points are exactly the set of irrational numbers whose continued fraction expansions (CFE) are eventually periodic. Due to a theorem of Lagrange, the set of numbers whose CFE is eventually periodic are exactly those numbers that are irrational solutions to quadratic equations with integer coefficients. Note that we do not count rational numbers as having an eventually periodic CFE, since their CFEs terminate at a finite length. Since the set of all quadratic equations with integer coefficients is countable, the set of fixed points to the map f is also countable. Since any rational number has a finite CFE, and the rational numbers are dense on the real line, the set of fixed points of f is also dense on the real line. This can be seen from the following argument. Using the standard notation from number theory,

$$[m_0, m_1, m_2, m_3, \ldots] \equiv m_0 + \cfrac{1}{m_1 + \cfrac{1}{m_2 + \cfrac{1}{m_3 + \cfrac{1}{\ddots}}}} \ , \tag{11}$$

let the CFE for some rational number r be given by $r = [m_0, m_1, \ldots, m_n]$. Now consider the fixed point w_0 described by some eventually periodic CFE. Since w_0 has an eventually periodic CFE, it is a fixed point of f^p for some p. To see this, we note that all fixed points w_0 of order p are solutions to equations of the (most general) form

$$O^{\mu_N} B O^{\mu_{N-1}-1} B O^{\mu_{N-2}-1} B \ldots B O^{\mu_0-1}(w_0) = w_0 \ , \tag{12}$$

where the μ_j are positive integers satisfying $\sum_{j=0}^{N} \mu_j = p$, with the important exception that μ_N can be zero. From the definitions of B and O, it is easy to prove that the CFE for w satisfying equation (12) is given by

$$w_0 = [\mu_0, \{\mu_1, \mu_2, \ldots, \mu_{N-1}, \mu_N + \mu_0\}] \ , \tag{13}$$

where the braces indicate periodicity of the numbers therein, e.g. $[a, \{b, c\}] = [a, b, c, b, c, b, c, \ldots]$. By choosing $N = n + 1$, and $\mu_j = m_j$ for $j = 0, \ldots, n$, we get all $n + 1$ coefficients in the continued fraction expansion of r. Now we may choose μ_N such that w_0 becomes arbitrarily close to r by letting μ_N be arbitrarily large, but finite. As μ_N increases, the relative importance of the terms following it in the CFE for w_0 decreases. Thus as μ_N increases the CFE for w_0 approaches that of r. Since rationals are dense on the real line, and any rational is arbitrarily well approximated by a fixed point, the fixed points are dense on the real line. Thus the fixed points of f form a dense countable set.

B. The Map is Chaotic

To show that these fixed points are chaotic, we show that the fixed points have a positive topological entropy. The topological entropy is defined in analogy with the thermodynamic entropy. It measures the number of states available on the set of fixed points. If we let the number of fixed points of the kth order map be denoted by $N(k)$, then the topological entropy H is defined by

$$H = \lim_{k \to \infty} \frac{1}{k} N(k) \ . \tag{14}$$

For systems with no chaos, $N(k)$ is either finite or grows as k^p for some finite p. Thus for nonchaotic systems, $H = 0$. To count the number of fixed points at order k, we note that f^k can be broken up into a string of m O's and $k - m$ Bs. Therefore any periodic orbit can be traversed by applying the O and B maps in the right order m and $k - m$ times, respectively. For any string of length k, the only associated fixed point equation having no solution is $O^k(w) = w$. Thus the total number of fixed points at order k is given by the number of possible strings of Bs and Os, save one, which is just $2^k - 1$. Plugging this into equation (14), the topological entropy is

$$H_u = \ln 2 \ , \tag{15}$$

where the subscript u reminds us that this is for the restricted map f which acts only on u, not v. Since the analysis of the v map (f^{-k}) is identical (because the fixed points are identical), and because the topological entropy is additive, we conclude that the topological entropy for the Farey map is

$$H_F = H_u + H_v = 2 \ln 2 \ , \tag{16}$$

and from the positivity of H_F we conclude that the map F is chaotic.

C. The Fixed Points are Nonattracting

Finally, a very simple argument shows us that the set of fixed points is nonattracting. Since the system is conservative, there can be no sinks or sources. Thus one direction must be attracting and the other repelling. A simple stability analysis shows that the u direction is the unstable (future invariant) direction, and v is the stable direction. To see this, we consider an aperiodic trajectory that starts out at some point u_0 within ϵ of a period p fixed point w_0, so that $u_0 = w_0 + \epsilon$. After p applications of the Farey map F, the new value of u_0 to first order in ϵ is

$$f^p(u_0) = f^p(w_0 + \epsilon) = w_0 + c_p\epsilon \ , \tag{17}$$

where

$$c_p = f'(w_1)f'(w_2)\dots f'(w_p) \ , \tag{18}$$

and $f^k(w_0) = w_k$, with the subscript taken modulo p. To calculate c_p, we look at the first derivative of f:

$$f'(u) = \begin{cases} 1 & , u \geq 2 \\ \dfrac{1}{(u-1)^2} & , u < 2 \, , \end{cases} \tag{19}$$

As noted above, any periodic orbit must bounce at least once, since $O^k(w) = w$ has no solutions. Therefore, there exists an i such that w_i is less than 2. Since for any such w_i, $f'(w_i) > 1$, it follows that $c_p > 1$, and the u direction is the unstable direction. We already know from conservation laws that v must be the stable direction, but since the v map is the time reverse of the u map, we see again that v must be the stable direction. A similar stability analysis would have also worked, and is equally as simple as the u map analysis.

We now know that the set of fixed points comprises a (countable, dense) set that is chaotic and nonattracting, and it is thus a repeller. In the next section, we show that this set is in fact a fractal set, making it a so-called strange repeller.

IV. THE FRACTAL GEOMETRY OF THE REPELLER

To explore the fractal nature of the repeller, we first focus on the reduced Farey map. We compose a histogram of the fixed points taken over all the orders up to and including order 14. One can clearly see from figures (1) and (2) that the distribution of fixed points is self-similar. In the limit, the full repeller will have the property that the histogram for the interval $u \in [n, n+1]$ is the same as for $u \in [n+1, n+2]$, only with twice as many points. This is a consequence of the fact that for a periodic orbit, the sequence $O^{n-1}B$ must occur somewhere in the expansion (12) for a fixed point to lie in the interval $[n, n+1]$. Thus, the probability of a fixed point lying in that interval is 2^{-n}, and we have the exponential fall off that is evident in figures (1) and (2).

This is our first glimpse at the fractal nature of the repeller. To explore this further, we may move up to the full Farey map, and plot the distribution of fixed points in the phase plane of u and v. As noted in the beginning of section III A, the set of fixed points in the plane is just the Cartesian product of the set of fixed points for the reduced map. Plotting this set for all fixed points up to and including order 8, we see in figure (3) that the repeller looks something like the product of two Cantor sets. Again, self-similarity is apparent.

It is clear now that the repeller is a strange repeller, i.e. a fractal set. To prove this, we calculate the information dimension of the repeller. The information dimension D_I is defined as

$$D_I = \lim_{\epsilon \to 0} \frac{\sum_{j=1}^{N(\epsilon)} p_j \ln p_j}{\ln \epsilon} \ , \tag{20}$$

where $N(\epsilon)$ is the number of boxes of side length ϵ needed to cover the phase space, and the p_j are the probabilities of being in the jth box for a typical trajectory. If we define $\mathcal{N} = 1/\epsilon$, and then multiply the top and bottom by a negative sign and consolidate terms, we find that

$$D_I = \lim_{\mathcal{N} \to \infty} \sum_j p_j \log_{\mathcal{N}} \frac{1}{p_j} = \lim_{\mathcal{N} \to \infty} H_{\mathcal{N}}(u) \ , \tag{21}$$

where $H_b(u)$ is the Shannon entropy in base b of the typical trajectory u over all time. Thus we have the relationship of D_I to information. For nonfractal sets, the information dimension gives an integer result which is the same as the regular (box-counting) dimension. For fractal sets, however, the result is not an integer. So by proving that D_I is not an integer for the repeller, we will have proven that the repeller is indeed a fractal.

Though it is possible to calculate the information dimension directly from the graph of figure (3), we may save ourselves the effort by working again with the reduced map. If the information dimension for the u map is D_I^u, then for the v map we have $D_I^v = D_I^u$, since the fixed points are the same for both maps. For the full Farey map, and thus the full repeller, we have $D_I^F = 2D_I^u$ from the additivity of information.

To calculate D_I^u, simply choose a "typical" initial condition, and begin applying the reduced map f. For extremely long times, almost any trajectory is typical. Alternatively, an ensemble average over many trajectories may be taken. Now partition the u axis into intervals of length ϵ, and count the frequency with which each site is visited to obtain the probabilities p_j. We may do this for any given choice of ϵ, so for several choices we may calculate the numerator and denominator of (20) separately and plot the result, as in figure (4). By fitting a line to the data, we obtain an estimate of D_I^u from the slope. Then twice this number is D_I^F, which for the author's calculation is

$$D_I^F = 1.75 \pm .01 \ .$$

This non-integer value for the information dimension conclusively proves that the discrete dynamics of the mixmaster universe is chaotic. For the continuum dynamics, however, we have proven nothing. We have very strong evidence now that we will reach the same conclusion, but a full numerical investigation would be necessary to confirm our suspicions. All of the tools that we have used to tackle the discrete problem will be useful for the continuous case, but the continuum dynamics is much more challenging numerically and it is for this reason that we omit it from this paper. Detailed calculations have been done elsewhere, and the result is remarkably close to the discrete approximation: the information dimension for the continuum dynamics was calculated as $D_I = 1.72 \pm .02$ by Cornish and Levin. This result proves that the mixmaster universe is indeed chaotic.

V. STRANGER STILL: HIDDEN FRACTALS IN THE REPELLER

In the course of studying the discrete mixmaster universe, we found a fractal set that has not yet been discussed in the literature, to the best of our knowledge.

The algorithm used by the author to generate the fixed points starts with order 1 fixed points, and then recursively finds the higher orders. To do this, the algorithm starts with the list $\{B, O\}$, and finds the fixed points of the associated map, i. e. solutions to $B(x) = x, O(x) = x$. The next generation of fixed points is calculated by acting B on the first order string, and appending the list with O acting on the first order string. Thus, the order for the second order fixed points is given by solving the associated equations to the list of strings $\{BB, BO, OB, OO\}$. Repeating, we see the kth order fixed points are found by first concatenating B and then O to the $(k-1)$th order string list and solving for the fixed points, as illustrated in table I. This is just the tensor product ordering structure. Alternatively, by identifying $B \to 0$ and $O \to 1$, the ordering for a given k is exactly the ordering of the binary numbers of length k. The fixed points are then ordered with the lesser of each pair of fixed points first for each string in the list. There are always only two solutions for each string, as the O^k maps are thrown out for each k. The list of all fixed points is then made by concatenating the lists as ordered by their respective values of k.

TABLE I: Strings generating the fixed points of order k for the Farey map

Order	*String*
k=1	B,O
k=2	BB,BO,OB,OO
k=3	BBB,BBO,BOB,BOO,OBB,OBO,OOB,OOO
k=4	BBBB,BBBO,BBOB,BBOO,BOBB,BOBO,BOOB,BOOO, OBBB,OBBO,OBOB,OBOO,OOBB,OOBO,OOOB,OOOO
⋮	⋮

Given this ordering, a natural question to ask is: what is the distribution of fixed points as a function of rank in the list? The answer is quite surprising, and is shown in figure (5). (Note the negative of the fixed points is plotted.) Although given the recursive ordering one might expect some type of self-similarity, one wouldn't expect *a priori* that the positive and negative roots would have such vastly different structure, or that the structure of the negative roots would exhibit strong dependence on the ordering while the positive roots don't. The appearance of a "band gap" structure is not unexpected given the histogram of figures (1) and (2). However, the self-similar "leaves" of the negative roots have no explanation as of yet. Figures (6) through (10) further explore this strange and puzzling phenomenon. Our bewilderment is compounded by the fact that figures (11) and (12) seem to imply that the distribution of negative roots is *exactly the same* as for the positive roots, albeit shifted up by $+1$. Indeed, there are no discernible differences with figures (1) and (3), respectively. Thus we expect that the structure in figures (5) through (10) should be symmetric about $u = 1/2$, which is clearly not the case.

Although the author is investigating this phenomenon, there are currently no further results to report.

VI. CONCLUSION

In this paper we have discussed the chaotic dynamics of a discretized version of the mixmaster universe. By proving that the unstable manifold of fixed points was a fractal set,

we have given an observer independent demonstration of chaos. The emergence of a strange, possibly new fractal associated with the ordering of the fixed points was mentioned, though no explanation for the structure was forthcoming.

VII. CONSULTED LITERATURE

An excellent starting point, as well as the primary source for most of this paper would be the article by Cornish and Levin, available as an `arxiv.org` eprint, number `gr-qc/9612066`. This article was preceded by a PRL by Cornish and Levin, available at `gr-qc/9605029`, which was the original announcement of the result. Motter and Letelier (`gr-qc/0011001`) purport to find a mistake in the work of Cornish and Levin, but it appears to the author that they are in fact *themselves* mistaken; a second opinion by someone more knowledgeable would much appreciated. In `gr-qc/9609072`, Berger et. al. present a new algorithm for solving the continuum dynamics of the mixmaster universe which could be useful. Strong evidence for chaos in the mixmaster universe was put forward by Chernoff and Barrow in Phys. Rev. Lett. **50**, 134 (1983). The mixmaster universe was first discussed by Misner in Phys. Rev. Lett. **22**, 1071 (1969). The subsequent discussion in chapter 30 of *Gravitation* by Misner, Thorne, and Wheeler is another good starting point. Ott's book *Chaos in Dynamical Systems* has a nice discussion of the information dimension, as well as the more general spectral dimensions and multifractals. *Deterministic Chaos in general relativity*, editors. D. Hobill, A. Burd and A. Coley, offers a somewhat dated but thorough discussion of just what the title says.

Acknowledgments

The author would like to thank Dan Finley for his patience and guidance with this project, and Kiran Manne for helping me find arcane *Mathematica* commands that allowed me to complete this project in a (somewhat) timely fashion.

Appendix A: *Mathematica* Code

This section displays the code used to generate the figures and results in this paper.

Preliminary Definitions

This defines the "Bounce" and "Oscillate" portions of the Farey Map. It also sets the directory where the saved files will be stored.

```
SetDirectory["/Users/steve/Desktop/solutions"];
b[x_] = 1/(x - 1);
o[x_] = x - 1;
```

Calculating the Solutions

Here we calculate the fixed points of the reduced Farey map up to order $pmax$. The solutions are stored in files labeled by a letter "s" and a number that corresponds to the order of the map. All solutions up to order "k" are in the file t"k".

```
pmin = 1;
pmax = 14;
{x} >> "f0"
{} >> "t0"
For[p = pmin, p  pmax, p++,
  bb = Flatten[ReadList["f" <> ToString[p - 1]]];
  ff = Flatten[Reap[Sow[o[bb]]; b[bb]], 3];
  ff >> "f" <> ToString[p];
  aa = Table[Solve[ff[[i]] == x, x], {i, 2^p}];
  DeleteCases[Flatten[x /. aa], x] >> "s" <> ToString[p];
  Flatten[Append[ReadList["t" <> ToString[p - 1]],
    ReadList["s" <> ToString[p]]]] >> "t" <> ToString[p];
] // Timing
```

Plotting the Histogram

This plots a histogram of the number of times a fixed point appears in a bin of width $rstep$ in the interval $[rmin, rmax)$.

```
<<Graphics`Graphics`

rmin=1;
rmax=5;
rstep=.001;
his=Select[<<t14,rmin<#<rmax&];

Timing[hcat=Table[i,{i,rmin,rmax,rstep}];
  Histogram[his, HistogramCategories -> hcat, ImageSize -> 72*8]]
```

Plotting the Strange Repeller

This plots the strange repeller on the intervals shown below.

```
UnsortedUnion[x_]:=Reap[Sow[1,x],_,#1&][[2]];
rep=Select[<<t8,1<#<5&];
rep1=UnsortedUnion[Flatten[rep]];
repeller=Flatten[Table[{rep1[[i]],rep1[[j]]},{i,Length[rep1]},
  {j,Length[rep1]}],1];

ListPlot[repeller, PlotRange->{{1,5},{1,5}},
  PlotStyle->PointSize[0.002], AspectRatio->1, ImageSize->72*8]
```

Calculating the Information Dimension

This code iterates a random trajectory about 2^{16} times and counts how many times it passes through each bin. Then the entropy is calculated. The plot of entropy vs. $\ln \epsilon$ yields a straight line, the slope of which determines the information dimension of the reduced map f. Twice this slope is the information dimension for the full Farey map. An error analysis is performed at the end.

```
<<Statistics‘DataManipulation‘
<<Statistics‘LinearRegression‘

transients = 100;
imax = 2^(16) + transients;
rmin = 1;
rmax = 41;
kmin = 3;
kmax = 10;
boot = Table[{0, 0}, {m, 2 (kmax - kmin) + 1}];
l = 1;
For[k = kmin, k  kmax, k += 1/2,
  seed = Random[] + 1;
  test = Table[seed KroneckerDelta[1, j], {j, imax}];
    For[i = 1, i < imax, i++,
      test[[i + 1]] = Which[test[[i]] < 2, b[test[[i]]],
        test[[i]]  2, o[test[[i]]]];
  newtest = Select[Drop[test, transients], rmin < # < rmax &];
  epsilon = 2^(-k);
  probs = BinCounts[newtest, {rmin, rmax, epsilon}]/Length[newtest];
  probs2 = DeleteCases[probs, 0];
  entropy = Sum[N[probs2[[i]] Log[probs2[[i]]]], {i, Length[probs2]}];
  boot[[l]] = {Log[epsilon], entropy};
  l++;
]//Timing
fitline = Fit[-boot, {1, x}, x];
Show[{ListPlot[-boot, PlotStyle->PointSize[0.02]], Plot[fitline, {x, 1, 8}]},
  PlotRange->{{1, 8}, {1, 10}},  ImageSize->72*8];
fitline
2 D[fitline, x]
Regress[-boot, {1, x}, x]
```

Another Unusual Fractal

By plotting the fixed points as a function of their position in the list,we find a new and unusual fractal structure that depends on both the nature of the map (and it's fixed points) and on the ordering with which the fixed points were calculated.

```
ListPlot[-<<t14,PlotRange->{-10,10},PlotStyle->PointSize[0.002],ImageSize->72*8];
neg=Select[<<t14,#<0&];
ListPlot[-neg,PlotRange->{0,10},PlotStyle->PointSize[0.002],ImageSize->72*8];
pos=Select[<<t14,#>0&];
ListPlot[pos,PlotRange->{0,10},PlotStyle->PointSize[0.002],ImageSize->72*8];
ListPlot[-<<s14,PlotRange->{-10,10},PlotStyle->PointSize[0.002],ImageSize->72*8];
neg=Select[<<s14,#<0&];
ListPlot[-neg,PlotRange->{0,10},PlotStyle->PointSize[0.002],ImageSize->72*8];
pos=Select[<<s14,#>0&];
ListPlot[pos,PlotRange -> {0,10},PlotStyle->PointSize[0.002],ImageSize->72*8]
```

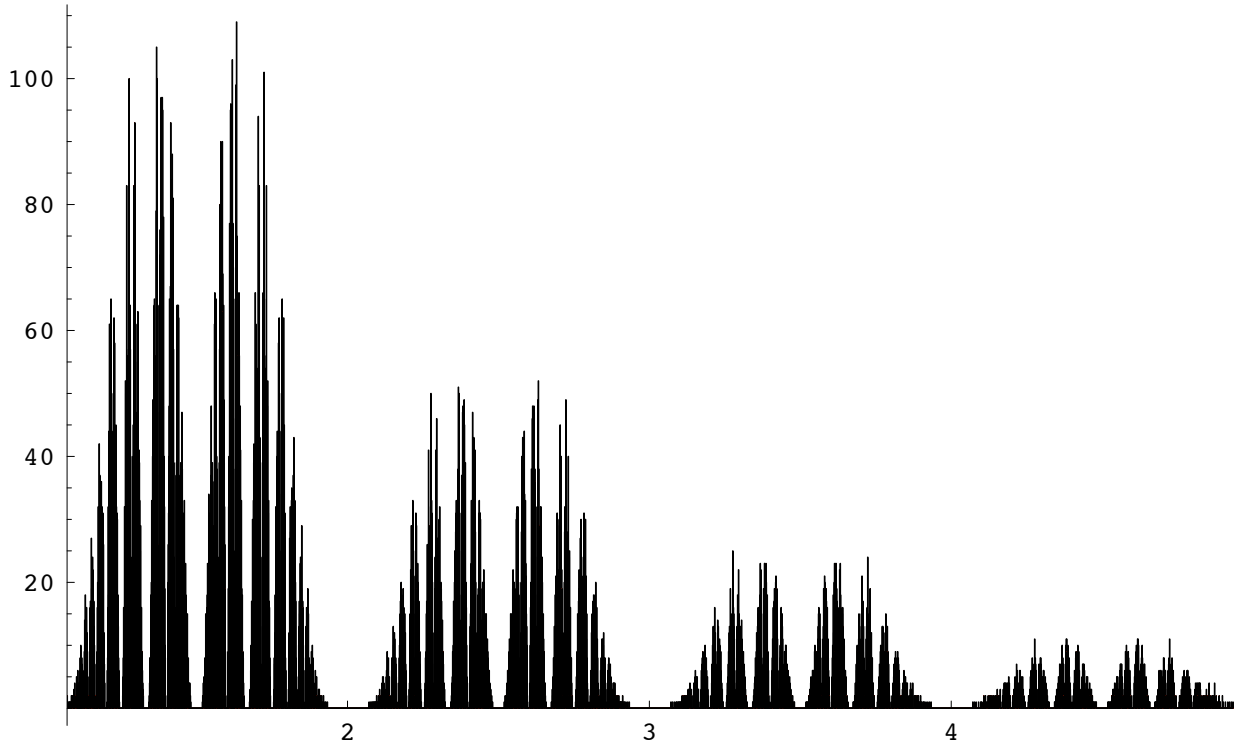

FIG. 1: Histogram of bin counts as a function of u for the fixed points of the reduced Farey map. All roots up to $k = 14$ inclusive are plotted.

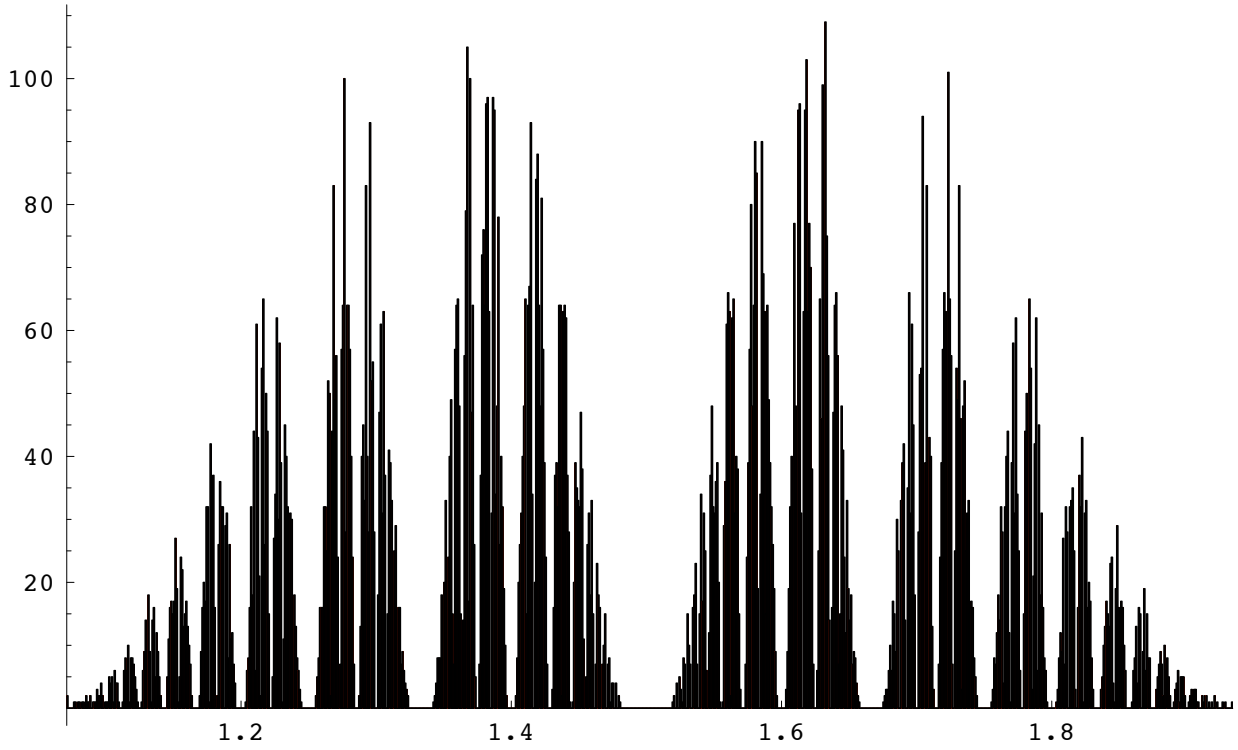

FIG. 2: Histogram of bin counts as a function of u for the fixed points of the reduced Farey map up to and including order $k = 14$.

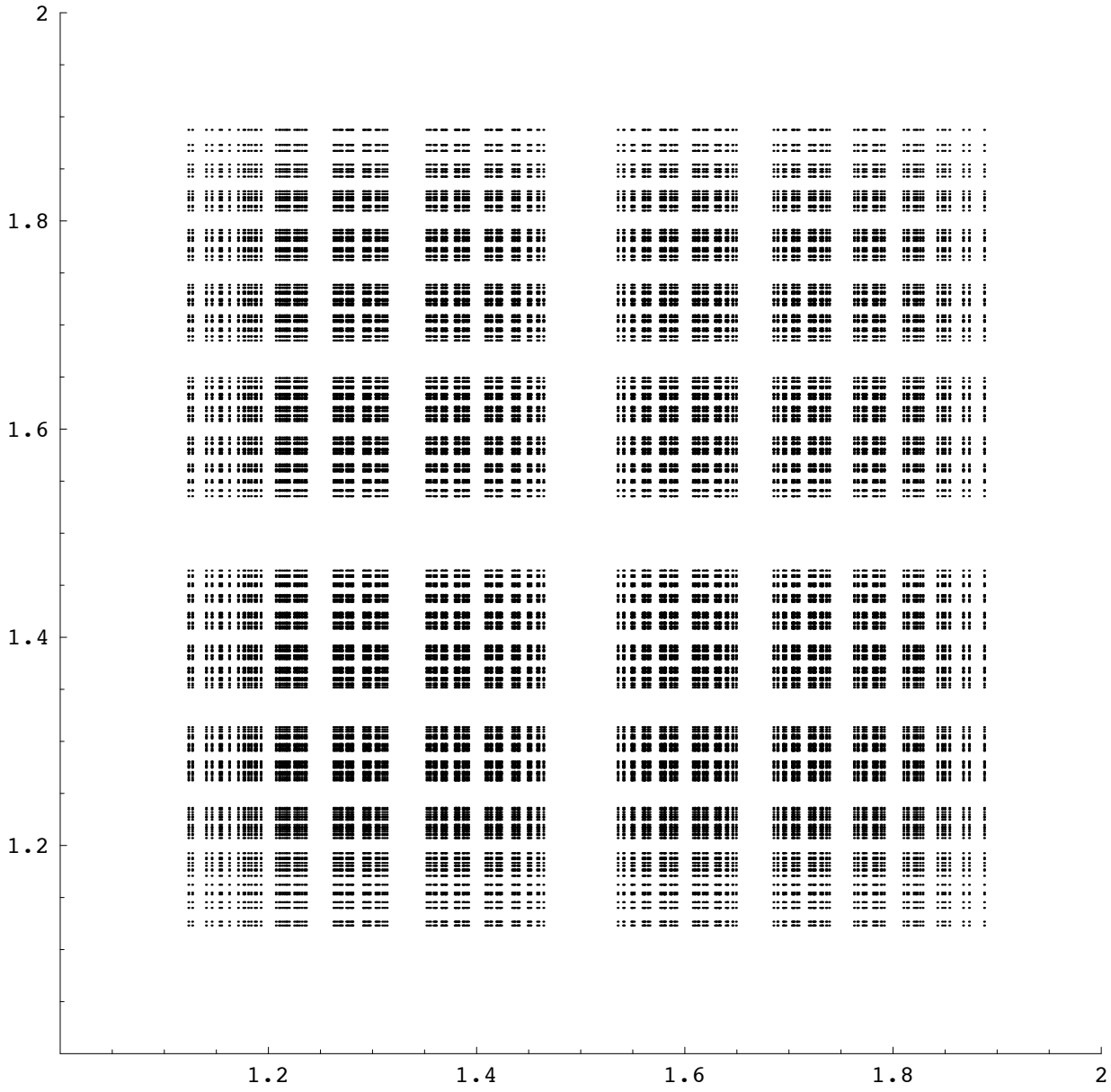

FIG. 3: Plot of the strange repeller in the u,v plane. All roots up to $k = 8$ inclusive are plotted.

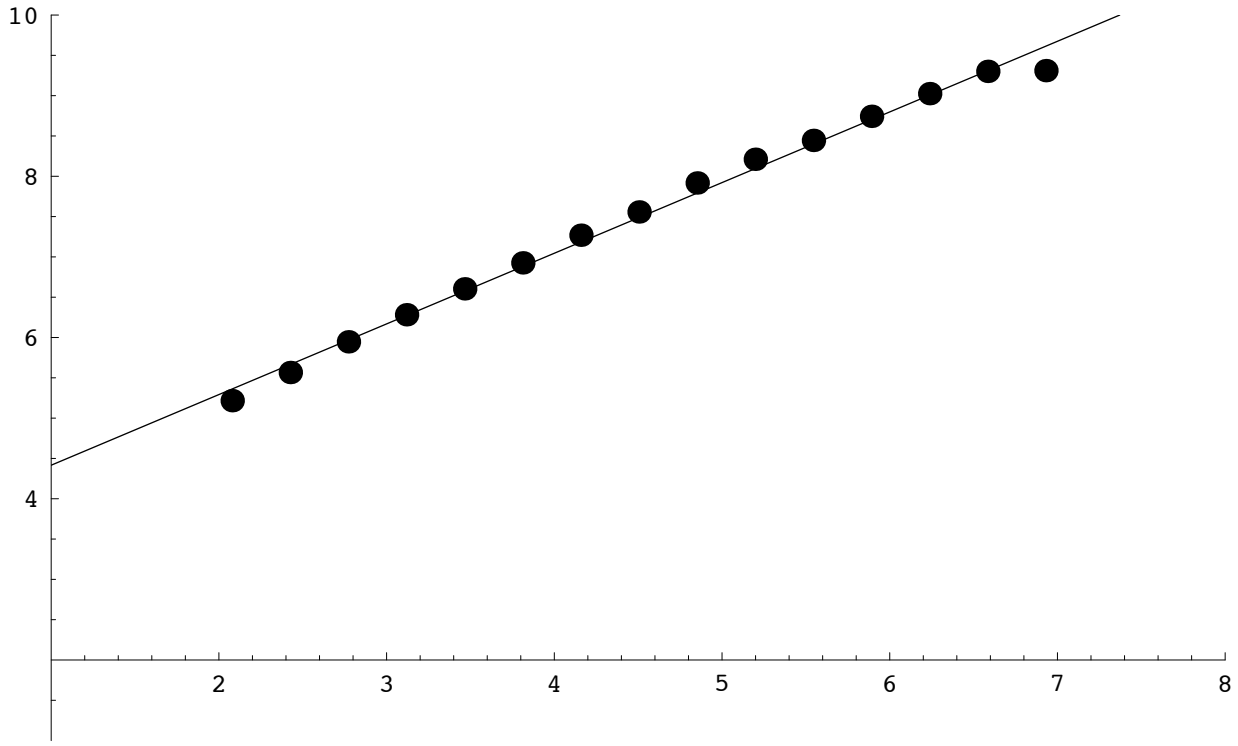

FIG. 4: Here is a plot used to calculate the information dimension of the reduced Farey Map. The information dimension D_I can be found by taking twice the slope of the best fit line.

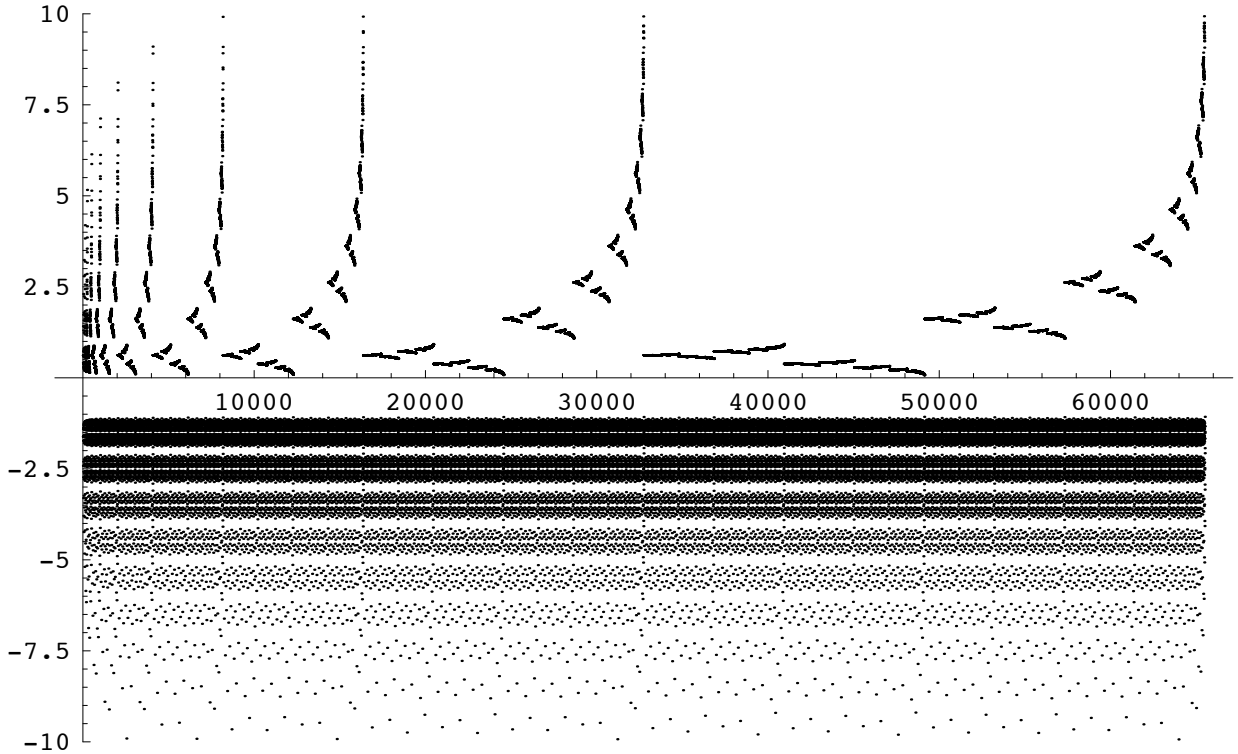

FIG. 5: Fixed points up to order $k = 14$ inclusive as a function of rank in the solution list. The negative of the fixed points has been plotted to emphasize the structure of the negative roots.

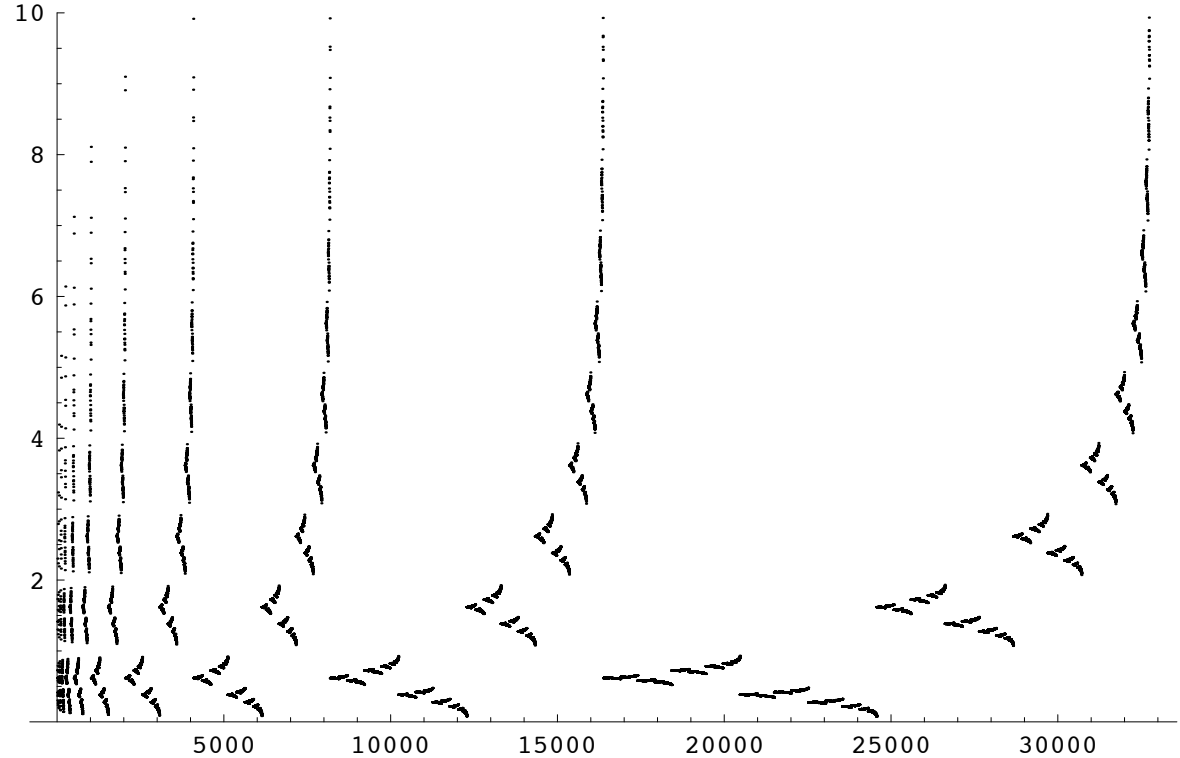

FIG. 6: Close up of the negative roots up to and including $k = 14$.

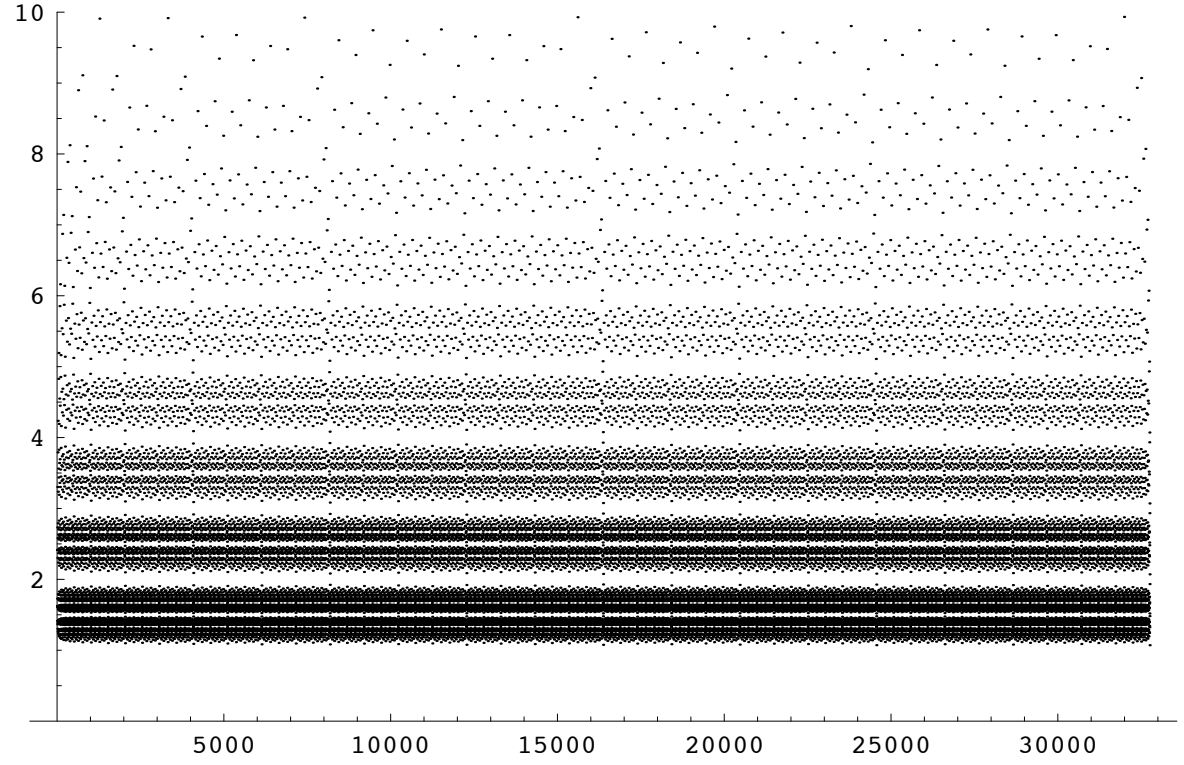

FIG. 7: Close up of the positive roots up to and including $k = 14$.

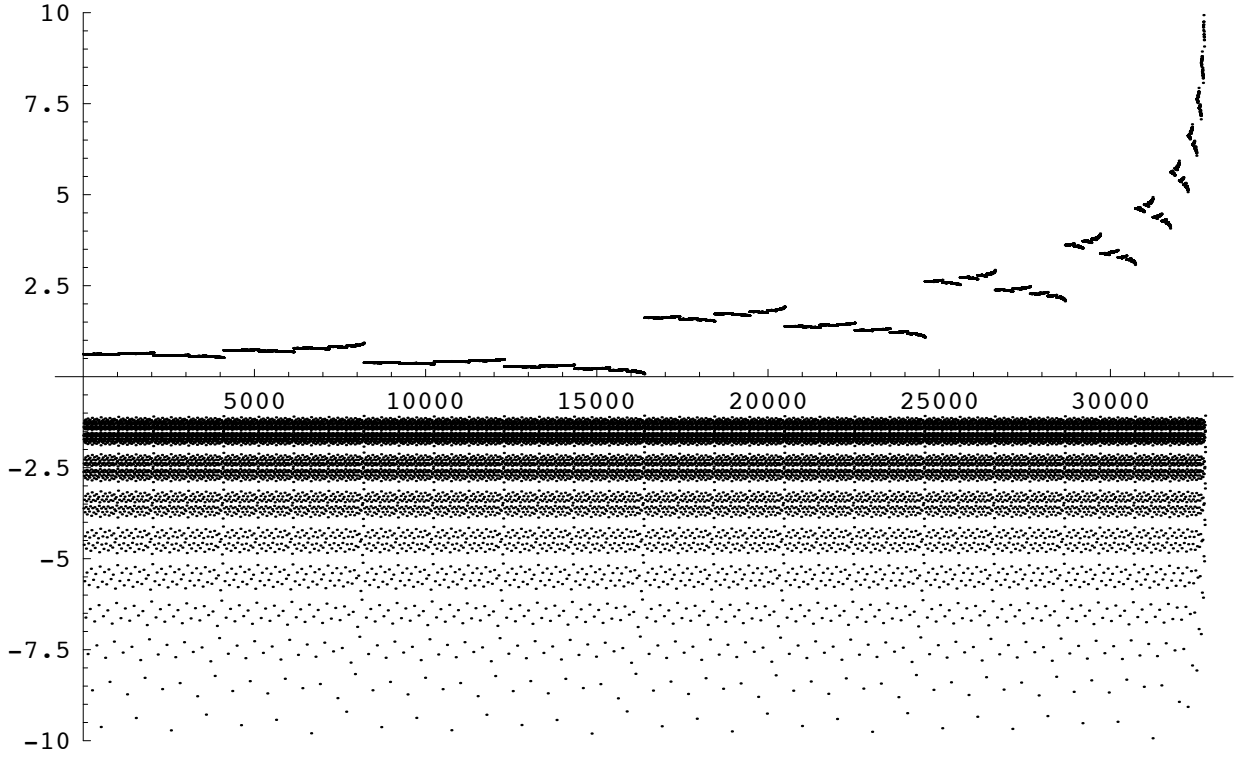

FIG. 8: Roots for just the $k = 14$ order fixed points.

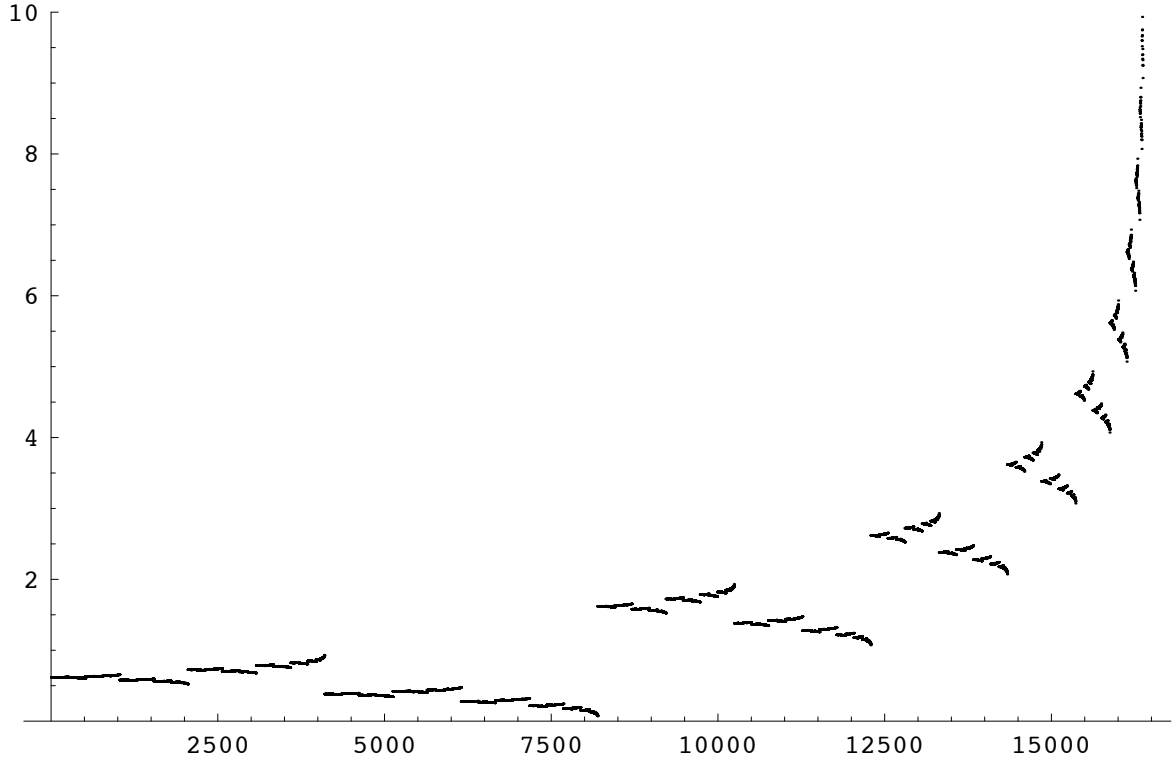

FIG. 9: Negative fixed points for the $k = 14$ map.

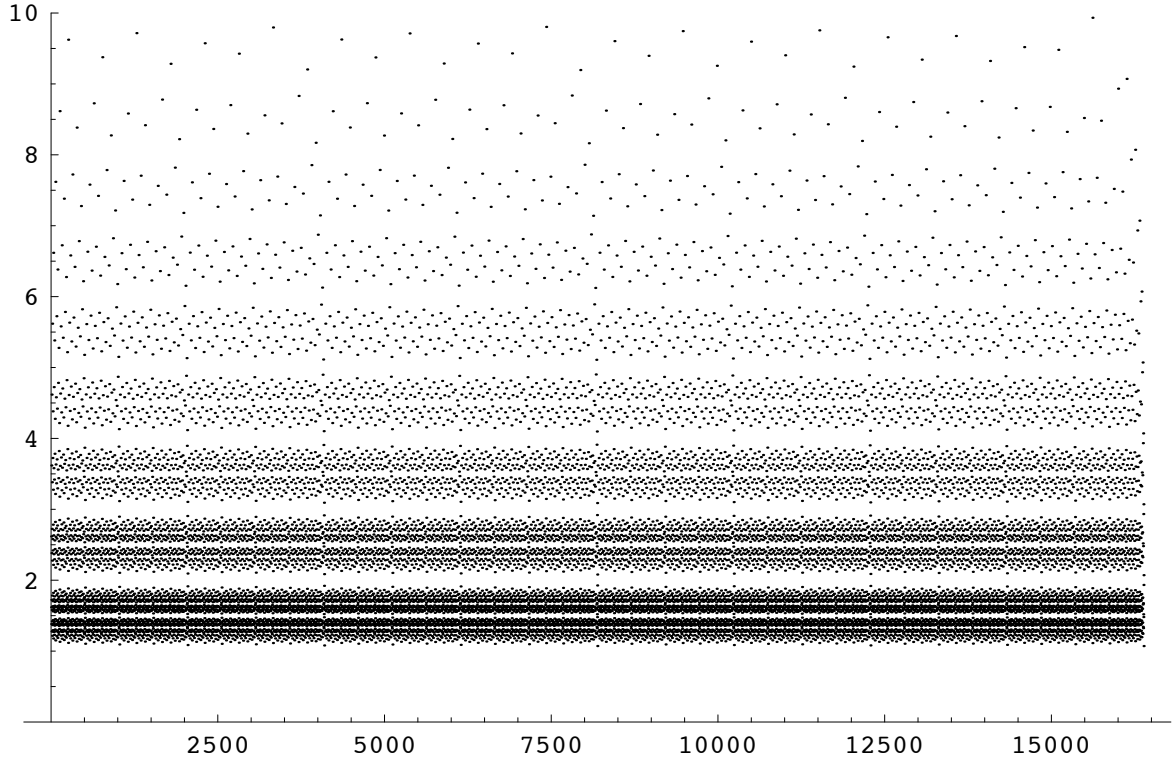

FIG. 10: Positive fixed points for the $k = 14$ map.

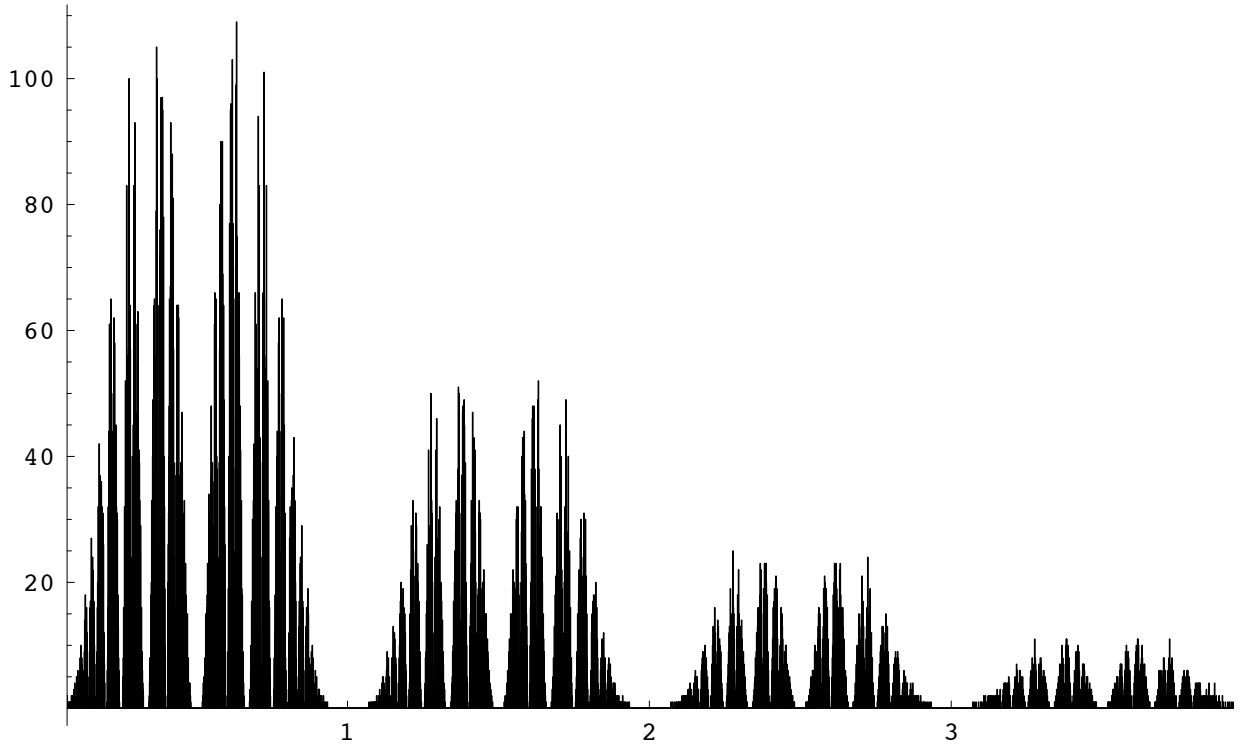

FIG. 11: Histogram of bin counts as a function of $-u$ for the fixed points of the reduced Farey map. Note the similarity to figure (1).

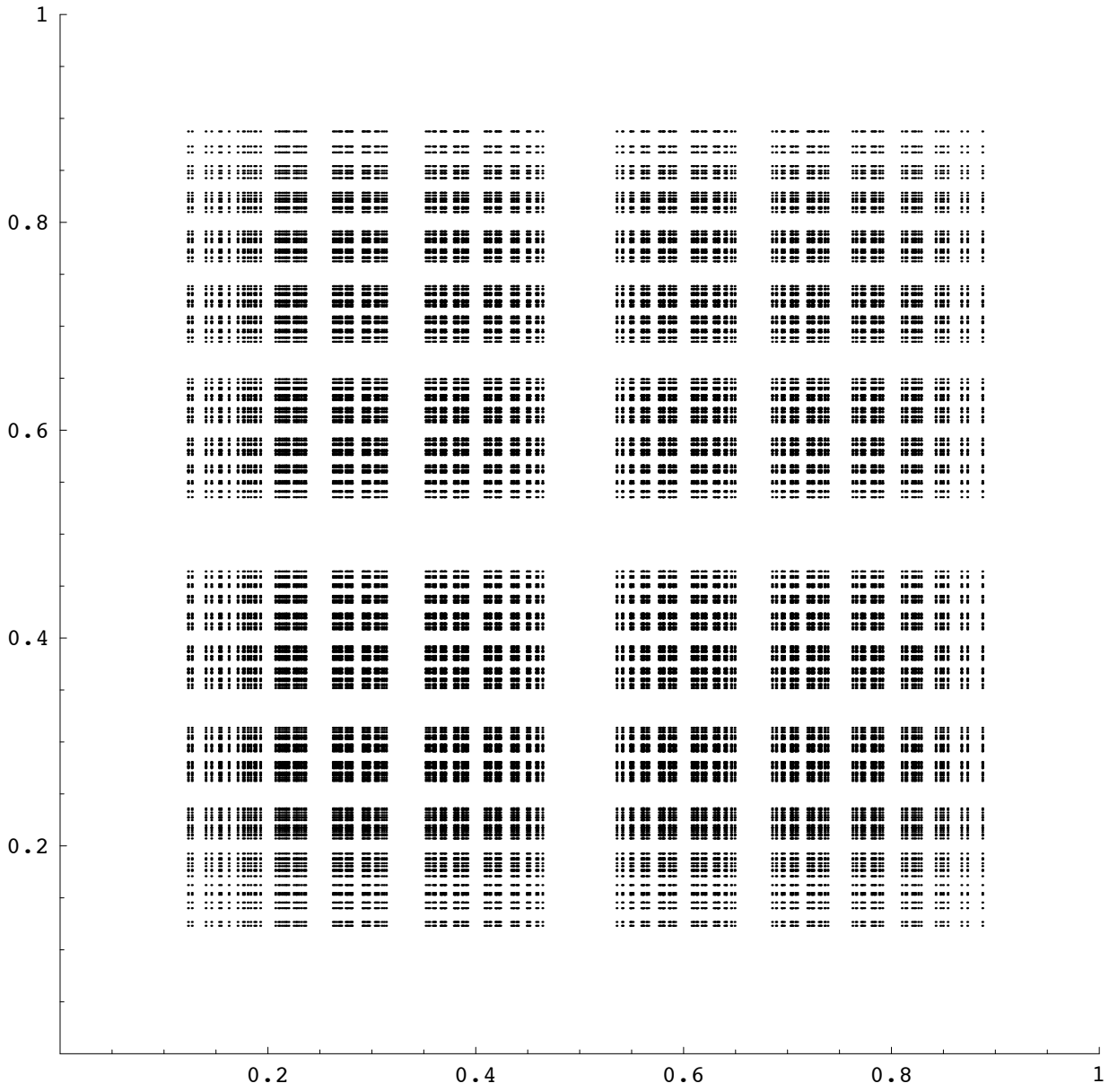

FIG. 12: Plot of the negative fixed points of the Farey map in the $-u$,$-v$ plane. Note the similarity to figure (3)